New spin models in ecology: super multi-stationarity and chaos

Ivan Sudakow[a,*], Sergey A. Vakulenko[b]

[a]*School of Mathematics and Statistics, The Open University, Milton Keynes, MK7 6AA, United Kingdom*
[b]*Institute for Problems in Mechanical Engineering of the Russian Academy of Science (IPME RAS) Bolshoy pr. V.O. 61, St.- Petersburg 199178, Russia*

Abstract

This manuscript introduces a novel spin model that captures the dynamics of ecological systems. We assume that these ecosystems consist of species whose ecological properties are completely determined by their discrete genotypes, and these genotypes are encoded by spin strings. We demonstrate that the Hamiltonian of this spin model can be derived naturally from classical models of population dynamics. Specifically, we establish a connection between the maximization of species abundance and the minimization of the Hamiltonian. The standard mean-field analysis reveals that the proposed spin model corresponds to the well-known Hopfield system, in general, characterized by asymmetric interactions. Remarkably, the resulting Hopfield system can possess an exponential number of local attractors, which, in the case of asymmetric interactions, may be complex. We term this characteristic "super multistationarity." We also demonstrate that super multistationarity combined with spontaneous symmetry breaking empowers populations to identify optimal genotypes. This adaptation process mirrors the search for solutions in a parallel computer.

Keywords: Ising model, spin, ecosystems, chaos, Hopfield system, environment

---

[*] Corresponding author
Email address: `ivan.sudakow@open.ac.uk` (Ivan Sudakow)

1. Introduction

The Ising and spin glass models have garnered significant attention in the field of statistical mechanics. To understand phase transitions, frustrated phenomena, and other effects related to these models, various methods have been developed, including mean-field theory, replica symmetric ansatz, cavity method, and others (see [1, 2] and the references therein). These models have found formidable applications in diverse areas such as neural network theory [3–7], computation theory [8], machine learning problems [9–13], as well as climate science [14–16] and biology [17–21]. These models have also been applied to describe multiagent systems capable of resolving hard combinatorial problems [22]. Moreover, they can be used to describe the formation of social groups [23]. Dynamics in such models can be described in various ways. The most well-known is the so-called Glauber dynamics; however, there are other interesting models as well [24].

In the context of ecology, spin models have been studied as presence-absence (PA) models [20]. In these models, each species is represented by a binary (spin) variable, with the i-th spin being assigned a value of 1 if the i-th species is present within an ecosystem, and -1 otherwise. Such models prove valuable in theoretically describing important phenomena, such as transitions from a niche mode to a neutral mode [19], and they can also be employed to model species biodiversity and spatial distribution (refer, for instance, to [20, 21]). Moreover, biologically motivated inverse problems can be explored by the Ising model (see [25, 26] and for a comprehensive overview, refer to [27]).

Consequently, there exists a compelling motivation to establish a theoretical link between these well-established classical models and the realms of evolutionary biology and ecology. E. Koonin and collaborators have undertaken this challenge in their research papers [28, 29], recognizing intriguing parallels between the observed phenomena in spin glasses and those encountered in evolutionary biology. These analogies provide a promising avenue for exploring and understanding the fundamental principles underlying both systems.

In this manuscript, we establish a new connection between classical ecological models, which have been proposed to describe species sharing the same resources [30, 31] and spin interaction models. We generalize classical population dynamics models by considering a Boolean genetic code and assuming that the species' growth rate function depends on the state $\mathbf{s}$ of this code. Through an averaging process, we demonstrate that the condition of achieving maximum species abundance over an extended time interval is equivalent to the minimization of a spin Hamiltonian, where spins correspond to binary genes. This connection highlights the underlying similarities and mathematical equivalences between ecological dynamics and spin models. In the case, where we are dealing with a single gene, the resulting Hamiltonian closely resembles the Ising model. Such a model can also be perceived as a PA model [19]. As we move to the case of multiple genes, a vector spin model emerges, bearing resemblance to more complex spin glass models [2]. We believe that this vector model is useful for accounting for the effects of gene regulation and for explaining evolution in an ecosystem under the influence of a changing environment.

For instance, consider the evolution from ancient rhinoceroses to woolly rhinoceroses during a period of climate cooling. In contrast to their contemporary counterparts, woolly rhinoceroses boasted elongated heads and bodies, coupled with shorter legs. Their elevated shoulders supported a robust hump, serving both as a platform for the animal's substantial front horn and as a fat reservoir crucial for winter survival in the expansive mammoth steppe. Given this, it is reasonable to anticipate the involvement of numerous genes in the transition from ancestral rhinoceroses to the woolly variety. Vector spin models provide a framework to elucidate the mechanisms driving successful adaptation amid cooling conditions (see Fig. 1).

1.1. Super multistationarity and complex dynamics in spin systems

Unlike presence-absence models, we employ spins in a distinct manner and pursue different objectives. Our primary aim is to unveil a novel adaptivity property, which we term '*adaptivity via super multistationarity*' of ecosystems, and to comprehend the interplay between genetics and ecology—particularly in response to changes induced by climate or other stressors.

Let us consider, for example, bacterial populations. They exhibit remarkable adaptability across vastly different environments. Various bacterial species demonstrate the ability to survive at diverse temperatures, often spanning extremes of both high and low ranges. They can thrive beneath ice or at depths of kilometers without access to oxygen. Additionally, organisms like plants are proficient at adapting to fluctuating surroundings, such as those characterized by chaotic changing weather patterns. The question then arises: How can we explain this exceptional adaptability displayed by ecosystems?

To make headway in tackling this challenging problem, this paper undertakes the following steps. By employing the standard mean-field approach, we derive a mean-field Hamiltonian from the given Hamiltonian. In the simplest case when we are dealing with a single gene (spin), the obtained Hamiltonian is similar to the standard Curie-Weiss model with an external field. The inverse temperature is proportional to the effective population size, and the field arises if a point mutation (the gene flip) affects adaptive properties, i.e. the growth function. A more intriguing scenario emerges when several genes are involved, leading to vector spins and vector magnetization. To investigate the equilibrium states of this vector model, it is convenient to examine the dynamical equations associated with this model.

We find that the resulting system for dynamics of magnetization is the well-known Hopfield system with continuous time and, in general, asymmetric interactions. The Hopfield system has received considerable attention [2, 3], and it has been shown to possess a remarkable property known as Universal Dynamical Approximation (UDA). Currently, there is no general theory of dynamical systems for dimensions above 2, except for monotone and gradient-like systems. The study of each specific system with complex behavior is a rather difficult problem. The approach based on UDA allows us to investigate entire classes of systems depending on parameters. This shows that there are families of dynamical systems with parameters $\mathbf{P}$, which exhibit universality in the sense that they can simulate any prescribed system of differential equations by adjusting $\mathbf{P}$.

For further insights into UDA, refer to [32], as well as [33–35] for related results on UDA in the context of the Hopfield system and similar models. This implies that, to a certain extent, this model can simulate all possible finite-dimensional dynamical systems, such as those defined by systems of differential equations. Furthermore, it can be demonstrated that these models possess a remarkable property known as "super adaptability", which is critical for their ability to successfully navigate and respond to various environmental challenges and changes [36]. Specifically, if we consider a spin dimension of N, they can support $\exp(cN)$ local attractors, where $c > 0$.

We suggest that the multistationarity property, coupled with the classical theory of phase transitions for spin systems, can help explain the formidable stability of the biosphere under environmental challenges, such as fast climate changes. A possible mechanism is explained in Fig. 1. The key question is how to explain adaptive evolution in many directions. For example, to adapt to cooling conditions, woolly rhinoceroses should evolve to elongate heads and bodies, shorten legs, and develop a hump. It is challenging to imagine mutations simultaneously leading to such variations in phenotype, affecting many different organism traits within the same time period.

In fact, Fisher's classic work in the 1920s demonstrated that the probability of such multidimensional mutations is exponentially small [37–39]. The analysis, based on the analogy with spin systems, and the obtained results illustrate how one can significantly facilitate this adaptation process.

1.2. Hypothesis: how to overcome the bottleneck

Let us propose a hypothesis based on our results, explaining how populations navigate through a bottleneck induced by a climate catastrophe. It can be demonstrated that, as a consequence, when resources decrease and the species growth function approaches the mortality rate, the coefficient defining the spin-spin interaction becomes large. This results in ferromagnetic effects, dividing the entire area into zones with differently directed spins. Since our spins have high dimensions due to organisms containing many genes, one can expect that at different spatial locations represented by point x, we have different independent attractors.

Returning to the language of populations, this implies that the entire species population splits into subspecies, each with unique adaptive properties. These properties vary among different subspecies. When the ecological situation improves (i.e., the growth function increases), migration and sexual mixing occur, leading to the formation of a single species encompassing all necessary adaptive features. This process can be likened to hysteresis. However, a crucial distinction from classical models of statistical mechanics is that the spin dimension may be large.

In physics, classical spin models can be interpreted as the discretized version of a microcontinuum model. Regarding ecological systems, here we neglect the effects of smooth diffusion transitions, considering, for example, that the tundra-forest transition is sharp: in each point, either a tundra or a forest. We believe that for plant ecosystems, this boundary effect is not significant: the areas of mixed habitats are small compared to homogeneous areas. Additionally, the spin model dynamics considered in the paper are Markovian. Therefore, we neglect the memory effects in spin dynamics.

The paper is organized as follows. In the next Section 2, we derive the spin model from well-known population dynamics models. Section 3 focuses on the mean-field equations. The main results are discussed in Section 4, where we describe the possible dynamical behavior of our models over large time scales. Concluding remarks are provided in Section 5.

2. The resource competition ecosystem model

In mathematical ecology, there exist fundamental models that describe ecosystems where numerous species (such as plankton or plants) compete for limited resources. The standard model [30, 40, 41] was introduced to address the so-called Plankton paradox.

Another seminal model in ecological studies is the MacArthur model, extensively discussed in [31]. It shares similarities with the standard model, albeit with linear growth rate functions and resource turnover coefficients. Additionally, a variant of the MacArthur model was proposed in [31], where turnover rates do not incorporate factors v_k. While our reduction to spin models can be applied similarly to all these models, for the sake of clarity, we focus on the standard model. However, we extend it to account for spatial diffusion (species migration):

$$\frac{\partial u_i}{\partial t} = d_i \Delta u_i + u_i(\phi_i(v) - \mu_i - \gamma_i u_i), \qquad i = 1, \dots, N_{sp}, \tag{1}$$

$$\frac{\partial v_k}{\partial t} = D_k(S_k - v_k) - \sum_{i=1}^{M} c_{ki}\, u_i\, \phi_i(v), \quad k = 1, \dots, n, \tag{2}$$

Here $u = (u_1, u_2, \dots, u_{N_{sp}})$ is the vector of species abundances, $u_i = u_i(x,t)$, $t > 0, x \in \Omega$, $v = (v_1, \dots, v_n)$ is a vector of resource amounts. The set $\Omega \subset \mathbb{Z}^d$, where $d = 2$, is a bounded subset of discrete lattice $\mathbb{Z}^d$, for example, a rectangle $[1 : L_1] \times [1 : L_2]$. In eqs. (1) Δ denotes the standard discrete Laplace operator, μ_i are the species mortalities, and γ_i are self-limitation parameters. In eqs. (2) the unknown function v_k is the amount of the resource of k-th type consumed by all ecosystem species, $D_k > 0$ are resource turnover rates, S_k is the supply of the resource v_k, $D_k v_k(S_k - v_k)$ is the supply rate for k-th resource and $c_{ik} > 0$ is the content of k-th resource in the i-th species. We consider general growth rate functions ϕ_j that are bounded, smooth and non-negative and increasing with respect to the resources: $\frac{\partial \phi_j(v)}{\partial v_k} \geq 0$ for all j, k.

We complement system (1), (2) by the following initial conditions

$$u(0) = \bar{u}(X), \quad v(0) = \bar{v}(X), \tag{3}$$

where

$$\bar{u}_i > 0,\ i = 1, \dots, N, \ \text{ and } \ 0 \leq \bar{v}_k \leq S_k, \quad k = 1, \dots, n. \tag{4}$$

We set the periodic boundary conditions

$$u_i(x + L_1, y, t) = u_i(x + L_1, y, t) = u_i(x, y + L_2, t) \quad (x, y) \in \Omega,\ t > 0 \tag{5}$$

$$v_k(x+L_1,y,t) = v_k(x+L_1,y,t) = v_k(x,y+L_2,t) \quad (x,y)\in \Omega,\ t>0. \tag{6}$$

2.1. *Simplified model involving genes*

We would like to take into account the genetic code and its evolution. For this purpose, we suppose that the growth function ϕ_i depends not only on the resources v but also on the genotype $s(x,t)\in \mathbb{S}^N = \{-1,1\}^N$, which can evolve in time.

To simplify the statement, we set the species number $N_{sp}=1$ assuming that we are dealing with different variations of the same species located at different points, so we are seeking for $u_1(x,t)=u(x,t)$. Then system (1), (2) becomes

$$\frac{\partial u}{\partial t} = d\Delta u + u(\phi(v,\mathbf{s}) - \mu - \gamma u), \tag{7}$$

$$\frac{\partial v_k}{\partial t} = D_k(S_k - v_k) - c_k\, u\, \phi(v,\mathbf{s}), \tag{8}$$

where $k=1,\ldots,n$, $\mathbf{s}=\mathbf{s}(x,\tau)$, τ is a slow time, $\tau=\epsilon t$, and $0 << \epsilon << 1$ is a parameter of the evolution rate. So, when we consider the dynamics defined by system (7),(8) one can assume that τ is fixed (frozen), i.e., ecological dynamics is much faster with respect to genetic evolution of $\mathbf{s}$.

2.2. *Asymptotics for large turnovers*

The system (7), (8) is complex and has primarily been studied using numerical methods [40, 41]. In certain cases, this system can be reduced to the well-investigated multispecies Lotka-Volterra system. It's noteworthy that this Lotka-Volterra system exhibits the UDA property. Therefore, this approach aids in analytically proving the existence of chaos for (7), (8), which was previously observed only in numerical simulations [40, 41]. This reduction is feasible when turnovers are large, i.e., $D_k \gg 1$ (see [42]). Consequently, v_k approximates the resource supplies S_k, indicating that almost all resources are utilized in the ecosystem. Following [42], we express v_k for large turnovers D_k via u. In fact, for large D_k one can set $v_k = S_k - \tilde{v}_k$, where for $\tilde{v}_k$ one has

$$\frac{\partial \tilde{v}_k}{\partial t} = D_k \tilde{v}_k - c_k\, u\, \phi(\bar{S} - \tilde{v}, \mathbf{s}), \tag{9}$$

where $k = 1, \dots, n$ and $\bar{S} = (S_1, ..., S_n)$. Then it is clear that $\tilde{v}_k = O(D_k^{-1})$ and we obtain an asymptotic solution

$$\tilde{v}_k = D_k^{-1} c_k u \phi(\bar{S}, \mathbf{s}) + O(D_k^{-2}). \tag{10}$$

Removing the small terms $O(D_k^{-1})$ in eq. (7), we obtain then the following equation, which involves u only:

$$\frac{\partial u}{\partial t} = d\Delta u + u(\phi_i(\bar{S}, \mathbf{s}) - \mu - \gamma u). \tag{11}$$

2.3. Averaging and maximum principle

We denote $\langle u \rangle$ the spatial average of u over Ω:

$$\langle u(\cdot, t) \rangle = |\Omega|^{-1} \sum_{x \in \Omega} u(x, t),$$

where $|\Omega| = L_1 L_2$ is the number of the location points x inside Ω.

It is well known that mutations are seldom. Therefore, we can choose a large time interval $[0, T]$ for averaging such that $T >> 1$ but $T << \epsilon^{-1}$. Following [42, 43] we use the time averaging over $[0, T]$:

$$\langle u(x, \cdot) \rangle_T = T^{-1} \int_0^T u(x, t) dt,$$

and we denote by

$$\langle\langle u(\cdot, \cdot) \rangle\rangle_T = T^{-1} \int_0^T \langle u(\cdot, t) \rangle dt$$

the result of averaging in space and time. Let us divide the r.h.s and the l.h.s of eq. (11) by u:

$$u^{-1} \frac{\partial u}{\partial t} = d u^{-1} \Delta u + \phi_i(\bar{S}, \mathbf{s}) - \mu - \gamma u. \tag{12}$$

We suppose that our species are not extinct, i.e.

$$u(x, t) > \delta_0 > 0 \quad \forall x \in \Omega, t > 0. \tag{13}$$

Such ecosystems are called permanent (ecologically stable)[44]. For a continual model, where x take real values and Δ is the standard Laplacian operator, we have [42]

$$\langle\langle (\log u(x, t))_t \rangle\rangle_T = \langle\langle \phi(\bar{S}, \mathbf{s}(x, t)) - \mu - \gamma u + d\nabla u^2 u^{-2} \rangle\rangle_T + O(T^{-1}). \tag{14}$$

In the space discrete case, a similar relation can be found. For simplicity, we proceed with the derivation of this relation for $1D$ case, where $x \in \mathbb{Z}$ are integers, and periodical boundary conditions (5) hold with $L_1 = L$. We have

$$\langle \Delta u u^{-1} \rangle = \sum_{x=1}^{x=L} \frac{u(x+1) - 2u(x) + u(x-1)}{u(x)}. \tag{15}$$

Eq. (15) gives

$$\langle \Delta u u^{-1} \rangle = \sum_{x=1}^{x=L} \frac{b(x) - b(x-1)}{u(x)}, \tag{16}$$

where $b(x) = u(x+1) - u(x)$. It is clear that due to periodicity

$$\sum_{x=1}^{x=L} \frac{b(x) - b(x-1)}{u(x)} = \sum_{x=1}^{x=L} \Big(\frac{b(x-1)}{u(x-1)} - \frac{b(x-1)}{u(x)} \Big).$$

Therefore, we obtain

$$\langle \Delta u u^{-1} \rangle = \sum_{x=1}^{x=L} \frac{(u(x) - u(x-1))^2}{u(x)u(x-1)}. \tag{17}$$

The right-hand side of this equation will be denoted further as $\langle \nabla u^2 u^{-2} \rangle$. In fact, the r.h.s. of (17) is a discrete analog of the corresponding term in the continual model. Moreover, let us note that under (13) for bounded u such that $\sup u(x,t) < C$ one has

$$\langle \langle \log u(x,t))_t \rangle \rangle_T < (C - \delta)/T = O(T^{-1}).$$

The boundedness of u can be shown by eq. (11). These estimates show that for large T eq. (14) gives

$$\langle \langle u(x,t) \rangle \rangle_T \approx \gamma^{-1} \langle \langle \phi(\bar{S}, \mathbf{s}(x,t)) - \mu + d \nabla u^2 u^{-2} \rangle \rangle_T + O(T^{-1}) = -\mathcal{H}(\mathbf{s}). \tag{18}$$

We see that the maximum abundance corresponds to the minimum of the Hamiltonian $\mathcal{H}(\mathbf{s})$. The function Φ equals

$$\Phi(\mathbf{s}) = \phi(\bar{S}, \mathbf{s}(x,t)) - \mu.$$

Here $\nabla u(x) = u(x) - u(x-1)$ can be considered as a discrete analog of the nabla operator ∇u.

2.4. Growth function representations

To find an explicit form for the Hamiltonian (18), we need relations for $\Phi(\mathbf{s})$ and u via $\mathbf{s}$. The growth function Φ can be considered as a fitness thus we can use different approximations for the fitness. Moreover, let us note that Φ and u are pseudo-Boolean functions of $\mathbf{s}$. The general form of the pseudo-Boolean functions of N variables $s_i \in \{-1, 1\}$ is known. It can be written down as a Boolean analog of the Fourier sum (a multilinear polynomial) [45]:

$$\Phi(\mathbf{s}) = \sum_{X \in [N]} \hat{F}(X)\chi_X(\mathbf{s}), \tag{19}$$

where $[N] = \{1, 2, ..., N\}$, the sum is taken over all subsets X of $[N]$ and

$$\chi_X(\mathbf{s}) = \prod_{i \in X} s_i.$$

Suppose there are no epistatic effects in gene regulation, which represents the simplest case. Then we have

$$\Phi(\mathbf{s}) = a_0 + \sum_{k=1}^{N} b_k s_k. \tag{20}$$

If we are dealing with a single gene, (19) gives

$$\Phi(s) = a_0 + bs, \tag{21}$$

where coefficients a_0 and b may depend on the resource $\bar{S}$:

$$a_0 = a_0(\bar{S}), \quad b = b(\bar{S}). \tag{22}$$

If we take into account linear and quadratic terms in (19) we obtain a fitness arising from the Fisher Geometric model with mutations investigated in [46]. In this case, we have

$$\Phi(\mathbf{s}) = a_0 + \sum_{k=1}^{N} b_k s_k + \frac{1}{2} \sum_{k=1}^{N} \sum_{l=1}^{N} b_{kl} s_k s_l, \tag{23}$$

with coefficients depending on $\bar{S}$ (as above). In recent decades, studies of fitness functions for genuinely existing organisms have commenced (see, for example, [47, 48]). These studies reveal the existence of numerous peaks, valleys, and ridges connecting peaks in fitness landscapes. Moreover, investigations into fitness landscapes in natural populations have demonstrated low fitness for intermediate phenotypes, indicating the presence of valleys in the fitness landscape. In the context of mimicry, it was found [48] that natural selection promotes genetic architecture preventing the expression of intermediate phenotypes. Close fitness peaks are separated by ridges, allowing for a drift from local peaks.

Certainly, it is impossible to obtain such complex landscapes with (20), (21). A more accurate representation, capable of approximating intricate fitness landscapes and taking into account complex gene regulation, is currently being explored in [49]:

$$\Phi(\mathbf{s}) = a_0 + \sum_{i=1}^{K} b_i Y_i(\mathbf{s}) \tag{24}$$

with

$$Y_i(\mathbf{s}) = \sigma\Big(\sum_{j=1}^{N} w_{ij} s_j - h_i\Big),$$

where b_i, w_{ij}, h_i are coefficients, $\sigma(u)$ is a monotone increasing sigmoidal function such that $\sigma(+\infty) = 1$ and $\sigma(-\infty) = 0$. The matrix $\mathbf{W}$ with the entries w_{ij} defines an interaction between genes.

2.5. Simplified Hamiltonian

Let us consider the simplest scalar case (21). To find u, we suppose that $d > 0$ is small. Then a rough approximation for u via Φ is $u(x) \approx \gamma^{-1}(\Phi(\bar{S}, \mathbf{s}(\mathbf{x})) - \mu)$ (under condition that $\phi(\bar{S}, \mathbf{s}(\mathbf{x})) > \mu$). We obtain then

$$\nabla u(x)^2 u(x)^{-2} \approx \frac{b(s(x) - s(x-1))}{(a_0 - \mu + bs(x))(a_0 - \mu + bs(x-1))}.$$

We can simplify this relation further supposing that $|b| << a_0 - \mu$ and $a_0 > \mu$ (this means that mutation effects are small). It gives

$$\nabla u(x)^2 u(x)^{-2} \approx \frac{b(s(x) - s(x-1))}{(a_0 - \mu)^2}.$$

By substituting this relation into (18), we find that the one dimensional Hamiltonian $\mathcal{H}(\mathbf{s})$ takes the Ising form:

$$\mathcal{H}(s(\cdot)) \approx b \sum_x s(x) - 2J_0 \sum_x s(x)s(x-1), \tag{25}$$

where the coupling coefficient J_0 is equal to

$$J_0 = db^2(a_0 - \mu)^{-2} \tag{26}$$

and terms independent of s are removed in (25). Note that this model is ferromagnetic, i.e. the species migration and gene transfer produce the ferromagnetic interaction in the spin model. The formula for J_0 involves basic genetic and ecological parameters: the migration rate d, the mortality rate μ, and the fraction $b^2(a_0 - \mu)^{-2}$, where b can be interpreted as a sensitivity of the fitness with respect to flip mutation $s \to -s$, whereas $a_0 - \mu$ is a difference between growth function and mortality rate.

In the $2D$ case the sum in (25) must be taken over all pairs of the nearest neighbors:

$$\mathcal{H}(s(\cdot)) \approx b \sum_x s(x) - J_0 \sum_{x,y \in E} s(x)s(y), \tag{27}$$

where E denotes the graph of spin interaction with the set of vertices $V = \Omega$, which in this case, contains edges corresponding to nearest neighbors. We can envision that species within this ecosystem interact with each other through a coupling term. This coupling term arises due to various interactions such as sexual mixing, migration, or other forms of interaction. Then we can have a more general coupling than via nearest neighbors.

The scalar model (27) can be interpreted as a presence-absence (PA) model [20]. In fact, suppose that the species u consists of two subspecies, with spatial densities $u_1(x)$ and $u_2(x)$, and only a single subspecies lives at each point x. Assume that genomes of these subspecies differ in a single gene $s \in \{-1, 1\}$ only, and u_1 corresponds to $s = 1$ whereas u_2 bears $s = -1$. Then the presence-absence of u_1 at x is equivalent to $s(x) = 1,\ s(x) = -1$, respectively.

Let us consider the case (20). A similar computation gives

$$\mathcal{H}(\mathbf{s}(\cdot))) \approx \sum_{x} \sum_{l=1}^{N} b_l s_l(x) - \sum_{x,y \in E} \mathbf{J}\mathbf{s}(x) \cdot \mathbf{s}(y) + \sum_{x} \Psi(\mathbf{s}(x)), \tag{28}$$

where $\mathbf{J}$ is the coupling matrix with the entries $J_{lk} = d(a_0 - \mu)^{-2} b_l b_k$ and

$$\mathbf{J}\mathbf{s} \cdot \tilde{\mathbf{s}} = \sum_{l,k=1,\dots,N,\ l \neq k} J_{lk} s_l \tilde{s}_k, \quad \Psi(\mathbf{s}) = \mathbf{J}\mathbf{s} \cdot \mathbf{s}.$$

In the case (24) one has

$$\mathcal{H}(\mathbf{s}(\cdot)) \approx const + \sum_{x,y \in E} \mathbf{J}(\mathbf{s}(x), \mathbf{s}(y)) + \sum_{x} \Psi_R(\mathbf{s}(x)), \tag{29}$$

where

$$\Psi_R(\mathbf{s}) = \sum_{i=1}^{K} b_i \sigma\Big(\sum_{j=1}^{N} w_{ij} s_j - h_i\Big),$$

and the coupling term $\mathbf{J}$ has a complex form:

$$\mathbf{J}(\mathbf{s}, \tilde{\mathbf{s}}) = d a_0^{-2} \sum_{l=1}^{K} b_l \big(Y_l(\mathbf{s}) - Y_l(\tilde{\mathbf{s}})\big)^2.$$

Note that similar coupling terms arise in multiagent systems describing the formation of social groups [23]. They possess a transparent interpretation: each entry of the spin vector can be regarded as a feature, so $\mathbf{J}(\mathbf{s}, \tilde{\mathbf{s}})$ measures the distance between the spin strings $\mathbf{s}$ and $\tilde{\mathbf{s}}$. This distance is a complex function of $\mathbf{s}$ and $\tilde{\mathbf{s}}$. This model is not tractable and we simplify the coupling term that gives

$$\mathcal{H}(\mathbf{s}(\cdot)) \approx const - J_0 \sum_{x,y \in E} \mathbf{s}(x) \cdot \mathbf{s}(y) + \sum_{x} \Psi_R(\mathbf{s}(x)), \tag{30}$$

where J_0 is a constant.

So, we see that fundamental ecological models for systems competing for resources [30, 31, 40] can generate these Hamiltonians when assuming that the growth rate function of species involved in resource competition depends on the genes $\mathbf{s}$. Then the quantity $-\mathcal{H}$ corresponds to the average species abundance over a long time period, during which the genes remain fixed. The minimum of the Hamiltonian means that species abundance is maximal. It is also possible to obtain the Hamiltonian through another approach, namely a natural variation

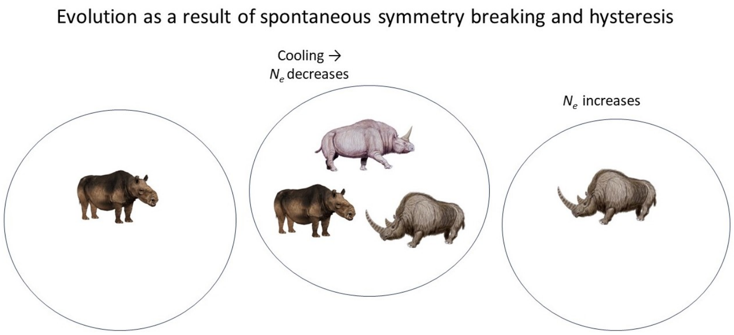

Figure 1: This illustration elucidates how segmentation and migration facilitate the evolution of species under climate variations, as exemplified by the transition from ancestral rhinos to woolly rhinos, specifically in the context of cooling. Initially, the population is homogeneous (as shown in the left panel, representing an area with a single species). As climate variations occur, the fragmentation parameter P_{frag} increases, leading to a potential "bottleneck" scenario. This increase triggers spontaneous symmetry breaking, resulting in the formation of distinct domains housing organisms with diverse traits. This phenomenon is facilitated by the modular structure of gene regulation. Consequently, various subspecies emerge, each adapted to specific habitats and displaying distinct features, such as the hump or longer body (refer to the middle panel, where the area domain is decomposed into three subdomains with three subspecies). The appearance of the hump represents a useful genetic innovation (feature A), and the emergence of a longer body represents another valuable trait (feature B). Subsequently, as the parameter P_{frag} rebounds and genetic mixing occurs (e.g., through sexual reproduction) within the entire habitat, a new organism emerges. This organism is well-suited to thrive in the new cold climate conditions, benefiting from both features A and B.

principle for ecological systems, as described in [31]. Note that if we wish to consider the effects of heterogeneity and external parameters, such as environmental temperature T_s or precipitation level P, we can consider a more general potential energy Φ, which involves parameters, for example, $\Phi = \Phi(s, x, T_s)$.

3. Mean field equations

Let us consider the Hamiltonian $\mathcal{H}_{sc}$ first. In order to apply the standard mean field approximation, we set $s(x) = m + \tilde{s}(x)$, where $m = \langle s \rangle$ represents the averaged magnetization (which does not depend on i due to translation invariance), and $\tilde{s}(x)$ denotes the fluctuations. We remove the quadratic fluc-

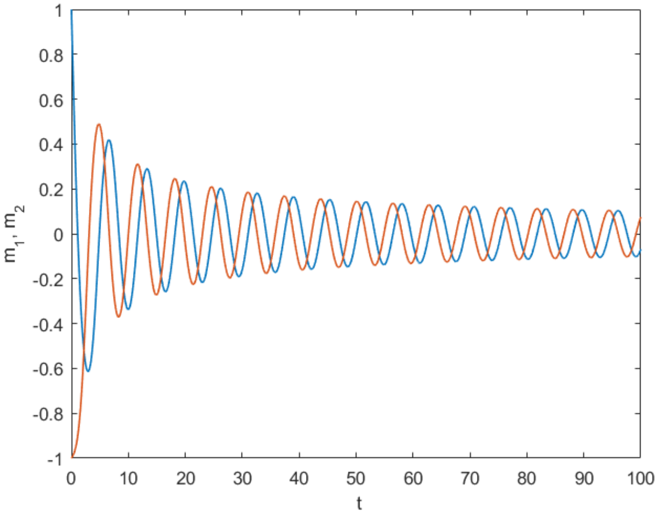

Figure 2: This plot shows an oscillating time evolution of magnetization for mean field equations. The spin dimension N is $N = 2$, the parameter values used are $h_1 = h_2 = 0.0$, $\beta = 1$ and the matrix $\mathbf{J}$ has the entries $J_{11} = J_{22} = J_{12} = 1, J_{21} = -1$.

tuation terms $\tilde{s}(x)\tilde{s}(y)$ and then this standard mean field approximation yields the following mean field Hamiltonian:

$$\mathcal{H}_{sc,MF} = M\frac{J_0 z m^2}{2} + \sum_{x\in\Omega}(J_0 z m - b)s(x), \tag{31}$$

where z is the number of neighbors (the coordinate number).

3.1. Scalar model

To simplify the subsequent statement, let us proceed with the derivation of (33) (the vector case equations can be obtained similarly). Consider the equation

$$d\log Z(m)/dm = 0, \tag{32}$$

where the Gibbs statistical sum has the form

$$Z = \sum_{s(\cdot)} \exp(-\beta M J z m^2/2)\exp\big(-\sum_{x}\beta(Jzm-b)s(x)\big),$$

where the sum is taken over all distributions $s(x),\ x \in \Omega$. We obtain

$$\log Z = -\beta M J_0 z \frac{m^2}{2} - M \log\cosh\big(\beta(J_0 z m - b)\big)$$

that by (32) gives

$$m = \tanh\big(\beta(J_0 z m - b)\big). \tag{33}$$

In the case of $b = 0$, where spin-flip does not alter the fitness (growth function), we obtain the following equation:

$$m = \tanh(\beta J_0 z m). \tag{34}$$

In biology, this case means that we consider a neutral situation when selection is absent. As the inverse temperature β increases, at $\beta = \beta_c$, we observe the Curie-Weiss transition. Mathematically, for $\beta J_0 z < 1$, equation (34) has a single root, while for $\beta J_0 z > 1$, it exhibits bistability with three roots.

Note that, according to [28, 29], the parameter β is proportional to the effective population size N_e. This means that the case of large populations, where genetic drift is small, corresponds to the low-temperatures in statistical mechanics. Conversely, in the case of small populations, where genetic drift is large, corresponds to high temperatures. The ferromagnetic effects in spin systems are analogous to fragmentation in an ecosystem. We thus conclude that the fragmentation effect depends on the parameter

$$P_{frag} = d b^2 (a_0 - \mu)^{-2} N_e. \tag{35}$$

The rough estimate of N_e by eq. (12) shows that for small $|b|$ and d the effective population size $N_e \propto (a_0 - \mu)\gamma^{-1}|\Omega|$. Let us note that $N_e \propto \int_\Omega u(x,t)dx$. The equilibrium spatially homogeneous solution of ((12) is $u_{eq} \approx (a_0 - \mu)\gamma^{-1}$. Finally, the fragmentation parameter can be estimated by

$$P_{frag} \approx d b^2 (a_0 - \mu)^{-1} \gamma^{-1} |\Omega|. \tag{36}$$

3.2. Vector model

In the vector case, by the same method, one can derive mean-field equations for the case of quadratic Hamiltonian given (28). We introduce magnetisation vector $\mathbf{m}$ with the components $m_l = M^{-1}\sum_x s_l(x)$ and fluctuations $\tilde{s}_l(x) = s_l(x) - m_l$. For simplicity, we suppose that only nearest neighbors interact, the coordinate number equals the constant z for all x. Then we compute as above and obtain the mean-field Hamiltonian

$$\mathcal{H}_{MF}(\mathbf{s}(\cdot)) \approx \sum_x \sum_{l=1}^N h_l^{eff}(\mathbf{m}) s_l(x) + z \sum_{l=1}^N \sum_{k=1}^N J_{lk} m_l(x) m_k(y), \tag{37}$$

where the effective field h^{eff} is defined by

$$h_l^{eff}(\mathbf{m}) = -b_l + z \sum_{k=1}^N J_{lk} m_k. \tag{38}$$

We can compute the Gibbs statistical sum

$$Z_{MF} = \sum_{s(x)\in\mathbb{S}^N} \exp\Big(- \beta \mathcal{H}_{MF}\Big)$$

in the mean-field approximation as above that gives

$$M^{-1} \log Z_{MF} = -\beta z M \sum_{k=1}^N \sum_{k=1}^N J_{kl} m_k m_l + \sum_{l=1}^N \log\cosh h_l^{eff}(\mathbf{m}).$$

Then for non-degenerate matrices J the mean-field equations can be written down as

$$m_k = \tanh\big(\beta(-b_k + \sum_{l=1}^N J_{kl} m_l)\big), \tag{39}$$

where $k \in \{1, \dots, N\}$.

4. Dynamics in vector case

To study possible bifurcations we consider the following dynamical equations, for which the system (39) determines the equilibrium equations

$$\frac{dm_k}{dt} = \tanh\big(\beta(-b_k + \sum_{l=1}^N J_{kl} m_l)\big) - m_k, \tag{40}$$

where $k = 1, \dots, N$.

This system is the well-known celebrated Hopfield model [3], which has been extensively studied. Firstly, it can be shown that this system is dissipative: there is a bounded absorbing set and thus the attractor always exists. For symmetric interactions, when the matrix $\mathbf{J}$ with the entries is symmetric, we obtain that all trajectories of (40) are convergent, i.e., magnetization $\mathbf{m}(t)$ approach to a solution (39) as $t \to \infty$. It is a consequence of a Lyapunov function existence for dynamics defined by (40) with symmetric $\mathbf{J}$. Note that we can have a number of stable equilibria.

In the general non-symmetric case, the system (40) exhibits the property of Universal Dynamical Approximation (UDA) (as defined in [32]). The general asymmetric case does not arise for linear and quadratic fitness functions defined by (20), (23), in particular, for the Fisher model, but this case may occur if we consider fitness (24) with a common non-symmetric matrix $\mathbf{W}$.

Currently, there is no general theory of dynamical systems (for dimensions above 2), with the exception of monotone and gradient-like systems. The study of each specific system with complex behavior is a rather difficult problem. The approach based on UDA allows us to investigate entire classes of systems depending on parameters.

To explain UDA property more formally, consider a finite-dimensional dynamical system defined by the following equations:

$$\frac{dq}{dt} = \tilde{Q}(q, \mathcal{P}), \quad \tilde{Q} \in C^1(B^n), \tag{41}$$

where B^n is an n-dimensional unit ball. Suppose the following condition holds:

Condition SS. *System (41) generates a global semiflow S^t, $t > 0$, defined on the n-dimensional closed ball $B^n \subset \mathbb{R}^n$ and having structurally stable (for example, hyperbolic) local attractors $\mathcal{A}_l$, $l = 1, \dots, k$.*

We have

Theorem 4.1. *Assume that dynamical system defined by (41) satisfies condition* **SS**. *Then for sufficiently large satellite numbers N_s there exist a matrix $\mathbf{J}$ and parameters b_k such that dynamical system defined by (40) has local attractors $\mathcal{B}_l$ topologically equivalent to $\mathcal{A}_l$. The restrictions of the semiflow S^t_H to $\mathcal{B}_l$ are orbitally topologically equivalent to the restrictions of semiflows S^t to $\mathcal{A}_l$.*

This means that dynamics (40) can simulate any prescribed structurally stable dynamics. Recall that structural stability is a fundamental property of dynamics, implying that the topological structure of trajectories of the system (41) on $\mathcal{A}_l$ remains unaffected by C^1-small perturbations of the vector field Q. Specifically, under small perturbations, hyperbolic fixed points remain unchanged and only shift slightly; they cannot transform into cycles, and vice versa—hyperbolic cycles cannot become points or chaotic attractors.

Structurally stable attractors can assume complex forms since structurally stable dynamics may exhibit chaos. If a hyperbolic invariant set Γ is attracting and is neither a fixed point nor a limit cycle, we refer to Γ as a chaotic (strange) attractor [50]. Hyperbolic sets possess a fundamental property known as *persistence*. Informally, this property implies that hyperbolic sets remain stable (robust) under sufficiently small, smooth perturbations (see [50] for details).

If the dynamics defined by the system (41) is not structurally stable, then the system (40) for magnetization can approximate trajectories defined by (41) over finite time intervals. This approximation property was initially demonstrated in the work of [51]. Moreover, this property has been established for many classes of systems, such as systems of chemical kinetics [52], Lotka-Volterra systems [53, 54], and even for general reaction-diffusion systems with two components [55].

Some numerical results of the dynamical effects are presented in Figs. (2),(3). In the Appendix, we state an algorithm to construct a system (40) with complicated large-time behavior, which can be controlled by a few parameters. It is important to note that the number of local attractors $\mathcal{A}_l$ can be exponentially large. This multistationarity effect will be further discussed in the subsequent subsection.

4.1. Multistationarity effects

The number of equilibria and local attractors generated by the dynamics (40) can be extremely large. This phenomenon of complex attractor emergence is attributed to the presence of feedback loops in the interaction structure and the modularity of that structure. The following assertion holds:

Proposition 4.2. *Under an appropriate parameter choice, system (40) with* $dim\ \mathbf{m} = N$ *nodes can have* 2^{cN} *chaotic or periodic structurally stable local attractors, where a constant* $c \in (0,1)$ *is uniform in* N *as* $N \to \infty$.

Proof. For the case of the rest point attractors, this claim is obvious. Let us take the diagonal matrix $\mathbf{J} = diag(a + a_1, a + a_2, ..., a + a_N)$, where $a_k > 0$ are parameters, $a > 0$. Let us set $b_k = 0$. Then the system of equations (40) decomposes into the following independent equations:

$$\frac{dm_k}{dt} = \tanh(2\beta(a + a_k)m_k) - m_k, \quad k = 1, ..., N. \tag{42}$$

So, for sufficiently large $\beta > \beta_k^*$ the k-th dynamical systems generated by equation (42) has two local attractors for rest points. The first attractor is close to -1, while the second attractor is close to 1. Hence, we have a total of 2^N attractors for the entire system formed by the set of equations (42).

A similar trick proves the assertion in the general case. According to Theorem 4.1, we can find a system (40) of dimension N_d (possibly, N_d is large but it is finite) with two low-dimensional local structurally stable attractors $\mathcal{A}_1$ and $\mathcal{A}_2$ with $dim(\mathcal{A}_i) < d_0$. We take M independent identical or almost identical such systems with these local attractors $\mathcal{A}_1$ and $\mathcal{A}_2$. The total system (40) involves MN_d unknowns and it is a union of these independent systems. Then this system has 2^M attractors that proves our assertion.

Comment 1: This proof demonstrates that bifurcations leading to multistationarity can occur in various ways. To gain a better understanding, let's consider the case of rest point attractors. New attractors can arise simultaneously if all the a_i values are equal ($a_1 = a_2 = ... = a_N$), or they can emerge sequentially if the a_i values are different. However, these phenomena can also occur for more complex types of attractors.

Comment 2: The property described by this claim can be interpreted as the super adaptability of our systems, arising from the exponentially large number of possible equilibria and spontaneous symmetry breaking in space-extended spin systems (corresponding to habitat fragmentation in biology).

Comment 3: As noted in the review [56], plants have evolved sophisticated systems to maintain mineral nutrient homeostasis, allowing them to cope with spatial and temporal variability in nutrient concentrations. These systems involve root architecture modification and the control of transporter expression in response to nutrient availability [56]. The expression and activities of genes coding for nutrient transporters, for instance, are finely regulated in multiple steps to adapt to a wide range of nutrient conditions [56]. We propose that such regulatory mechanisms can be described by complex attractors in gene expression dynamics. Our assertion regarding the formidable multistationarity in variants of spin system attractors can contribute to explaining how evolution has achieved such intricate regulatory mechanisms

Explaining the existence of such complex multicellular organisms supporting sophisticated regulatory systems remains a profound challenge in the field of biology [28, 29]. As early as 1930, Fisher demonstrated through his FGM model that positive mutations impacting multiple features in organisms simultaneously are exceedingly improbable [37]. This problem was subsequently investigated by H. Orr (for a comprehensive perspective, refer to [38]). Genomics data suggest that the evolution of organisms more intricate than bacteria may not necessarily have been driven by adaptive processes [28, 29].

By employing spin models and building upon the insights from claim 4.2, we can propose a physically and biologically plausible mechanism to address this challenge (refer to Fig. 1 and its corresponding comment). Let's consider a scenario where an organism needs to adapt to a new and demanding environment, requiring the acquisition of distinct features denoted as $F_1, F_2, ..., F_K$. The probability of a mutation generating all these necessary features concurrently is exceedingly low. However, it is reasonable to posit that under harsh conditions, the fragmentation parameter P_{frag} defined by (35) becomes significant, leading to the occurrence of phase transitions and ecosystem fragmentation.

This parameter is inversely proportional to $(a_0 - \mu)^2$, where $a_0 - \mu$ determines the population growth rate and can depend on the resource supply $\bar{S}$ and other ecological parameters. One can suppose that this coefficient decreases as the environment becomes more challenging.

Leveraging the significant multistationarity property highlighted in claim 4.2, we can anticipate that the entire habitat might fragment into subdomains, each potentially supporting a distinct subspecies (labeled as $1, 2, ..., K$). These subspecies may possess the requisite features $F_1, ..., F_K$, respectively. As these better-adapted organisms emerge, the population size N_e increases, leading to the dissolution of this fragmentation. Subsequent sexual mixing can then facilitate the emergence of a well-adapted organism encompassing all the necessary traits.

It's worth noting that there might be an alternative mechanism that doesn't necessarily rely on spontaneous symmetry breaking and fragmentation. Specifically, we could consider a more gradual evolution, where the organism acquires features like F_1, followed by F_2, and so forth (in any order).

The difference between these approaches lies in the timing of transitions and the rate of evolution, which could be particularly crucial during rapid environmental changes. The first option functions akin to a parallel computer, while the second resembles a conventional evolutionary process. Note that in spin systems, spin waves (magnons) exist, and these can be utilized for data processing [57]. In ecology, such waves can be interpreted as migration waves, driving the formation of new species. In certain cases, this formation process is very fast, as found in [58]. The evolution of complex features in plants was recently investigated in [59] using network methods, and it was shown that evolution rates could vary significantly for different species and situations.

5. Concluding remarks

In this paper, it is demonstrated that by incorporating Boolean genes into basic population dynamics models (which can be viewed as spins), the maximization of species abundance is equivalent to the minimization of a spin Hamiltonian. When only a single gene influences the species' growth function, a model similar to the Ising-like model is obtained.

However, if we consider a multigene control of the growth function, a vector spin Hamiltonian arises. Under the standard mean-field assumptions, this leads to the Hopfield system with non-symmetric interactions for magnetization. This system can exhibit chaotic behavior and demonstrate formidable multistationarity, meaning it can have a significant number of local attractors. The presence of this property plays a vital role in enabling ecosystems to attain and maintain super adaptability, which is essential for their resilience and ability to thrive in diverse and changing environments.

In this context, we do not take into consideration stochastic transitions between different local attractors due to internal and external noises. Additionally, we assume that the number of spins is fixed. The renowned mathematician, M. Gromov highlighted the idea that such transitions inevitably lead to the destruction of any biosystem with fixed parameters. This concept was further developed in [60], where it is demonstrated that gene evolution and the emergence of new genes can stabilize unstable biosystems. This leads us to consider a growing spin network as a general model for evolution, wherein the inclusion of new genes and the exploration of diverse gene interactions can greatly impact the adaptation and stability of ecological systems.

By interpreting ecological dynamics through the framework of spin Hamiltonians, we unveil striking parallels between the principles of physics and the intricate dynamics observed in ecological communities. Moreover, our research contributes to the broader series of works [32, 36, 55, 61] on Universal Dynamical Approximation (UDA) by examining its implications within the realm of statistical mechanics. The models exhibiting UDA properties possess the remarkable ability to simulate any finite-dimensional dynamics with a desired level of accuracy. This further highlights the potential of spin-based models to capture the complexity and richness of real-world ecological systems.

Let us note some similarities and differences with previous works. The model described in [24] focuses on long spin chains, where evolution oscillates between two processes resembling asexual and sexual reproduction. The line-graph operator from [24] can be viewed as an asexual process, while the recombination mechanism mirrors sexual reproduction. This allows for the depiction of alternating sexual-asexual reproduction. In our paper, we explore ecosystems where reproduction can take various forms; all genetic effects are encapsulated within the growth function.

The dynamics introduced in [23] elucidate the formation and dissolution of social groups. The formation of a social group within a large society mirrors the fragmentation of an ecosystem into subsystems to some extent. Similar to [23], our work employs spin strings, which may extend considerably in length. However, unlike the model in [23], which introduces the probability of forming an entire social group, our model's fragmentation arises from interactions between nearest spins, akin to classical Ising-type models. This process allows for an energy interpretation via a Hamiltonian. Ecological fragmentation of this nature can be depicted in a static model without delving into detailed dynamics.

CRediT authorship contribution statement

Ivan Sudakow: Conceptualization, Methodology, Funding acquisition, Writing – original and review & editing, Supervision, Validation. Sergey A. Vakulenko: Software, Formal analysis, Methodology, Writing – original draft, Visualization.

Declaration of Competing Interest

The authors declare that they have no known competing financial interests or personal relationships that could have appeared to influence the work reported in this paper.

Acknowledgements

We thank the Referees for interesting and useful comments.

I.S. gratefully acknowledges support from the Division of Physics at the National Science Foundation (NSF) through Grant No. PHY-2102906. Part of this research was performed while I.S. was visiting the Institute for Mathematical and Statistical Innovation (IMSI), which is supported by the NSF Grant No. DMS-1929348. This research was also supported in part by NSF Grant No. PHY-1748958, Gordon and Betty Moore Foundation Grant No. 2919.02, and the Kavli Foundation. S.V. is supported by a grant from the National Institutes of Health (NIH) 2R01 OD010936. The results of sections 4 and 5 were obtained within the state assignment of the Ministry of Science and Higher Education of the Russian Federation for IPME RAS (project No. 124040800009-8).

Appendix

In this Appendix, we show how, given a prescribed dynamical system, to obtain a spin system with a similar dynamics. As an example, we consider the Rössler system (similarly, we can simulate any quadratic system, and in turn, quadratic systems can simulate all possible dynamical systems):

$$\frac{dv_1}{dt} = -v_2 - v_3, \tag{A1}$$

$$\frac{dv_2}{dt} = v_1 + av_2, \tag{A2}$$

$$\frac{dv_3}{dt} = b + v_3(v_1 - c), \tag{A3}$$

where a, b, c are parameters. This system exhibits a very rich behavior when we vary these parameters: convergent, periodic and chaotic. The main trick is to transform this system into a slow-fast spin system one with additional variables. The first step is as follows. We introduce a small parameter $\gamma > 0$, a slow time $\tau = \gamma t$ and transforms (A1)- (A2) as follows:

$$\frac{dv_1}{d\tau} = \gamma^{-1} \tanh(\gamma(-v_2 - v_3 + v_1)) - v_1, \tag{A4}$$

$$\frac{dv_2}{d\tau} = \gamma^{-1} \tanh(\gamma(v_1 + av_2 + v_2)) - v_2. \tag{A5}$$

For bounded trajectories the right-hand sides of (A1) and (A4) differ by a term, which is $O(\gamma^2)$. Further, we approximate the term v_3v_1 via auxiliary fast variables. First, we use the identity $4v_3v_1 = v_+^2 - v_-^2$, where $v_\pm = v_3 \pm v_1$. By the

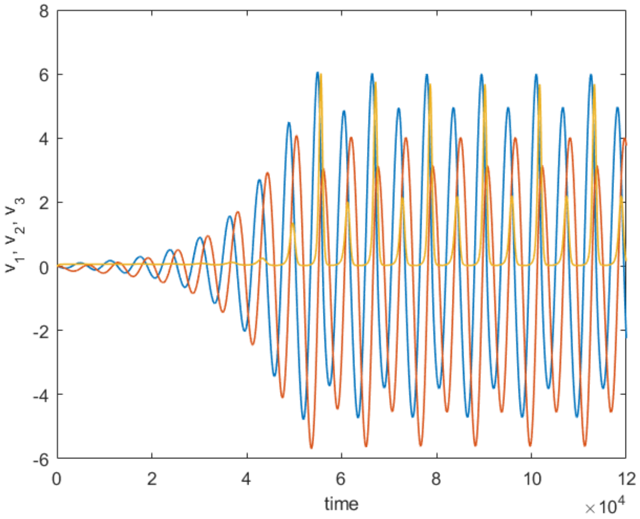

Figure 3: This plot shows a complex time evolution of magnetization for mean field equations. The spin system is constructed by the algorithm stated in the Appendix to simulate the Rössler system exhibiting a rich variety of large time regimes. Here the Rössler system with parameters $a = 0.2, b = 0.2$ and $c = 3$ is simulated, the parameter $\gamma = 0.001$. The spin number is 103, the matrix $\mathbf{J}$ corresponds to a spin interaction graph, where we have 3 nodes (centers) interacting with other 100 nodes (satellites) while the satellites do not interact with each other. This graph can be viewed as a simplified representation of real-world biological interaction graphs. This also illustrates the temporal evolution of magnetization for centers. Computations are by the program Ode45 in Matlab on time interval $I = [0 : 120]$. The accuracy of simulation is computed as $L_2(I)$-norm on the differences between the numerical trajectories of the Rössler system and the trajectories of the spin simulation (divided by the L_2-norm of the trajectories of the Rössler system). That accuracy is 0.046.

least mean squares, we can obtain an approximation

$$z^2 \approx \sum_{j=1}^{N_a} X_i \tanh(z - h_i) \tag{A6}$$

on a compact interval $[-R, R]$, where $R(a, b, c) > \max(|v_3(t)| + v_1(t)|)$, where v_3, v_1 are trajectories of the Röossler system (since this system is dissipative, such a constant R exists). Here h_i are thresholds located uniformly: $h_i = R + i(2R/N_a)$ and X_i are coefficients to adjust. Having X_i we represent $v_3 v_1$ as

$$v_3 v_1 \approx \sum_{j=1}^{N_a} \frac{X_i}{4}\Big(\tanh(v_3 - v_1 - h_i) - \tanh(v_3 + v_1 - h_i)\Big). \tag{A7}$$

Now we introduce additional fast variables $w_i^{\pm}$ satisfying equations

$$\frac{dw_i^{\pm}}{d\tau} = \gamma^{-1}\Big(\frac{X_i}{4}\tanh(v_3 \pm v_1 - h_i) - w_i^{\pm}\Big). \tag{A8}$$

Then we can rewrite (A3) as follows:

$$\frac{dv_3}{d\tau} = \gamma^{-1}\tanh\big(\gamma \sum_{i=1}(w_i^- + w_i^+ + v_3)\big) - v_3. \tag{A9}$$

Finally, we obtain the system of equations (A4), (A5), (A9) and (A8) which has the form of (40) for an appropriate matrix $\mathbf{J}$ and coefficients b_k.

The outcomes of this algorithm's operation are illustrated in Fig. 3.

References

[1] M. Talagrand, Mean Field Models for Spin Glasses.Vol I and Vol II, Springer, 2011.

[2] M. Talagrand, Rigorous results for the hopfield model with many patterns, Probability theory and related fields 110 (2) (1998) 177–275.

[3] J. J. Hopfield, Neural networks and physical systems with emergent collective computational abilities, Proceedings of the National Academy of Sciences 79 (8) (1982) 2554–2558.

[4] E. Gardner, B. Derrida, Optimal storage properties of neural network models, J. Phys. A: Math. Gen. 21 (1988) 271–284.

[5] D. Sherrington, S. Kirkpatrick, Solvable model of a spin-glass, Physical Review Letters 1792 (1975) 35.

[6] M. Shcherbina, B. Tirozzi, On the rigorous solution of gardner's problem, Comm. Math. Phys. 234 (3) (2003) 383–422.

[7] E. Jaynes, Information theory and statistical mechanics, Physical Review 106 (1957) 620.

[8] C. Moore, S. Mertens, The Nature of Computation, Oxford University Press, 2011. `doi:10.1093/acprof:oso/9780199233212.001.0001`.
URL `http://www.oxfordscholarship.com/view/10.1093/acprof:oso/9780199233212.001.0001/acprof-9780199233212`

[9] V. M. Poulsen, S. DeDeo, The cultural transmission of tacit knowledge, Journal of The Royal Society Interface 19 (2022) 2022–02238. `doi:https://doi.org/10.1098/rsif.2022.0238`.

[10] R. Louie, K. Kaczorowski, J. Barton, M. Chakraborty, A.K.and McKay, Fitness landscape of the human immunodeficiency virus envelope protein that is targeted by antibodies., Proceedings of the National Academy of Sciences 115 (2018) E564–E573. `doi:https://doi.org/10.1073/pnas.1717765115`.

[11] B. Daniels, D. Krakauer, J. Flack, Control of finite critical behaviour in a small-scale social system., Nature Communications 8 (2017) 1–8.

[12] E. Lee, Partisan intuition belies strong, institutional consensus and wide zipf's law for voting blocs in us supreme court., Journal of Statistical Physics 173 (2018) 1722–1733.

[13] G. Stephens, W. Bialek, Statistical mechanics of letters in words, Physical Review E 2010, 81, 81 (2010) 066119.

[14] A. J. Majda, B. Khouider, Stochastic and mesoscopic models for tropical convection, Proceedings of the National Academy of Sciences 99 (3) (2002) 1123–1128. `arXiv:https://www.pnas.org/doi/pdf/10.1073/pnas.032663199`, `doi:10.1073/pnas.032663199`.
URL `https://www.pnas.org/doi/abs/10.1073/pnas.032663199`

[15] Y.-P. Ma, I. Sudakov, C. Strong, K. M. Golden, Ising model for melt ponds on arctic sea ice, New Journal of Physics 21 (6) (2019) 063029. `doi:10.1088/1367-2630/ab26db`.
URL `https://dx.doi.org/10.1088/1367-2630/ab26db`

[16] I. Sudakow, M. Pokojovy, D. Lyakhov, Statistical mechanics in climate emulation: Challenges and perspectives, Environmental Data Science 1 (2022) e16. `doi:10.1017/eds.2022.15`.

[17] V. R. Nareddy, J. Machta, K. C. Abbott, S. Esmaeili, A. Hastings, Dynamical ising model of spatially coupled ecological oscillators, Journal of The Royal Society Interface 17 (171) (2020) 20200571. `doi:10.1098/rsif.2020.0571`.

[18] S. Zakany, S. Smirnov, M. C. Milinkovitch, Lizard skin patterns and the ising model, Phys. Rev. Lett. 128 (2022) 048102. `doi:10.1103/PhysRevLett.128.048102`.
URL `https://link.aps.org/doi/10.1103/PhysRevLett.128.048102`

[19] C. K. Fisher, P. Mehta, The transition between the niche and neutral regimes in ecology, PNAS 111 (2014) 13111–13116.

[20] S. Manel, H. C. Williams, S. J. Ormerod, Evaluating presence-absence models in ecology: The need to account for prevalence, Journal of Applied Ecology 38 (2001) 921–931.

[21] J. Elith, et al., Presence-only and presence-absence data for comparing species distribution modeling methods, Biodiversity Informatics 15 (2020) 69–80.

[22] M. A. Javarone, Solving optimization problems by the public goods game, Eur. Phys. J. B 171 (2017). `doi:10.1140/epjb/e2017-80346-61`.

[23] M. A. Javarone, D. Marinazzo, Evolutionary dynamics of group formation, PLoS ONE 12(11) (2017) e0187960.

[24] M. A. Javarone, J. A. O' Connor, Dynamics of spin models under line graph operator, Proc. Roayal Soc. A 477 (2021) 20210282.

[25] F. Morcos, A. Pagnani, B. Lunt, A. Bertolino, D. S. Marks, C. Sander, R. Zecchina, D. Onuchic, T. Hwa, M. Weigt, Direct-coupling analysis of residue coevolution captures native contacts across many protein families, Proc. Natl. Acad. Sci. USA 108 (2011) E1293–E1301.

[26] M. Weigt, R. A. White, H. H. Szurmant, J. A. Hoch, T. Hwa, Identification of direct residue contacts in protein-protein interaction by message passing, Proc. Natl. Acad. Sci. USA 106 (2009) 67–72.

[27] H. C. Nguyen, R. Zecchina, J. Berg, Inverse statistical problems: from the inverse ising problem to data science, Advances in Physics 66 (2017) 197–261.

[28] M. I. Katsnelson, Y. Wolf, , E. V. Koonin, Towards physical principles of biological evolution, Phys. Scripta 93 (4) (2018) 3001.

[29] Y. I. Wolf, M. I. Katsnelson, E. V. Eugene V. Koonin, Physical foundations of biological complexity, PNAS 115 (37) (2018) E8678–E8687.

[30] J. Huisman, F. Weissing, Biodiversity of plankton by species oscillations and chaos, Nature 402 (6760) (1999) 407–410.

[31] R. Marsland III, W. Cui, P. Pankaj Mehta, The minimum environmental perturbation principle: A new perspective on niche theory, The American Naturalist 196 (3) (2020).

[32] T. Tao, On the universality of the incompressible euler equations on compact manifolds, Discrete and Continuous dynamical systems 38 (3) (2018). doi:10.3934/dcds.2018064.

[33] S. Vakulenko, A system of coupled oscillators can have arbitrary prescribed attractors, Journal of Physics A: Mathematical and General 27 (7) (1994) 2335.

[34] S. Vakulenko, Dissipative systems generating any structurally stable chaos, Advances in Differential Equations 5 (7-9) (2000) 1139–1178.

[35] S. A. Vakulenko, O. Radulescu, Flexible and robust networks, Journal of bioinformatics and computational biology 10 (02) (2012).

[36] J. Reinitz, S. Vakulenko, I. Sudakow, D. Grigoriev, Robust morphogenesis by chaotic dynamics, Scientific Reports 13 (1) (2023) 7482. doi:10.1038/s41598-023-34041-x.
URL https://doi.org/10.1038/s41598-023-34041-x

[37] R. Fisher, J. Bennett, H. Bennett, The Genetical Theory of Natural Selection: A Complete Variorum Edition, OUP Oxford, 1999.

[38] H. A. Orr, The genetic theory of adaptation: a brief history, Nat. Rev. Genet. 6 (2) (2005) 119–127. doi:10.1038/nrg1523.
URL http://www.nature.com/doifinder/10.1038/nrg1523

[39] I. Sudakow, J. Reinitz, S. A. Vakulenko, D. Grigoriev, Evolution of biological cooperation: an algorithmic approach, Scientific Reports 14 (1) (2024) 1468. doi:10.1038/s41598-024-52028-0.
URL https://doi.org/10.1038/s41598-024-52028-0

[40] J. Huisman, F. Weissing, Biological conditions for oscillations and chaos generated by multispecies competition, Ecology 82 (10) (2001) 2682–2695. doi:10.1890/0012-9658(2001)082[2682:BCFOAC]2.0.CO;2.

[41] J. Huisman, F. Weissing, Biodiversity of plankton by species oscillations and chaos, Nature 402 (6760) (1999) 407–410, copyright - Copyright Macmillan Journals Ltd. Nov 25, 1999; Last updated - 2012-11-14; CODEN - NATUAS.

[42] I. Sudakow, S. A. Vakulenko, M. Pound, D. Kirievskaya, Biome stability and fragmentation under critical environmental temperature change, Applied Mathematical Modelling 114 (2023) 189–204.

[43] J. Hofbauer, K. Sigmund, Evolutionary Games and Population Dynamics, Cambridge University Press, 1998.

[44] S. A. Vakulenko, I. Sudakov, S. V. Petrovskii, D. Lukichev, Stability of a planetary climate system with the biosphere species competing for resources, Phys. Rev. E 103 (2021) 022202. `doi:10.1103/PhysRevE.103.022202`.

[45] R. Donnell, ANALYSIS OF BOOLEAN FUNCTIONS, Cambridge University press, 2014.

[46] S. Hwang, S.-H. Park, J. Krug, Genotypic complexity of fisher's geometric model, Genetics 206 (2016) 1049–1079. `doi:https://doi.org/10.1534/genetics.116.199497`.

[47] I. G. Szendro, M. F. Schenk, J. Franke, J. Krug, J. de Visser, A. G. M., Quantitative analyses of empirical fitness landscapes, J. Stat. Mech. Theory Exp. 2013 (01) (2013) P01005. `arXiv:1202.4378`, `doi:10.1088/1742-5468/2013/01/P01005`.

[48] M. Arias, Y. Yann le Poul, M. Chouteau, R. Boisseau, N. Rosser, M. Thery, V. Llaurens, Crossing fitness valleys: empirical estimation of a fitness landscape associated with polymorphic mimicry, Proc. R. Soc. B 283 (2016) 0391–0400.

[49] P. Jiang, J. Reinitz, M. Kreitman, The effect of mutational robustness on the evolvability of multicellular organisms and eukaryotic cells, Journal Evolutionary Biology 36 (2023) 906–924.

[50] D. Ruelle, Elements of differentiable dynamics and bifurcation theory, Elsevier, 2014.

[51] K. Funahashi, Y. Y. Nakamura, Approximation of dynamical systems by continuous time recurrent neural networks, Neural Networks 6 (1993).

[52] M. Savageau, E. Voit, Recasting nonlinear differential equations as s-systems: a canonical nonlinear form, Mathematical Biosciences 87(1) (1987).

[53] B. Hernandez-Bermejo, V. Fairen, Lotka- volterra representation of general nonlinear systems, Mathematical Biosciences 140(1) (1997).

[54] Kozlov, V., S. Vakulenko, On chaos in lotka–volterra systems: an analytical approach, Nonlinearity 26 (2013) 2299.

[55] S. Vakulenko, I. Sudakov, Complex bifurcations in Bénard-Marangoni convection, Journal of Physics A: Mathematical and Theoretical 49 (42) (2016) 424001. `doi:10.1088/1751-8113/49/42/424001`.

[56] I. Aibara, K. Miwa, Strategies for optimization of mineral nutrient transport in plants: Multilevel regulation of nutrient-dependent dynamics of root architecture and transporter activity, Plant Cell Physiol. 55(12) (2014) 2027–2036.

[57] A. V. Chumak, et. al., Advances in magnetics: Roadmap on spin-wave computing, IEEE TRANSACTIONS ON MAGNETICS 58 (2022).

[58] S. Lamichhaney, et. al., Rapid hybrid speciation in darwin's finches, Science 359 (2018) 224–228.

[59] A. B. Leslie, M. L., Quantifying the complexity of plant reproductive structures reveals a history of morphological and functional integration, Proc. R. Soc. B 290 (2023) 20231810.

[60] S. Vakulenko, D. Grigoriev, Instability, complexity, and evolution, Zap. Nauchn. Sem. POMI, 2008 360 (2006) 31–69.

[61] I. Sudakow, S. A. Vakulenko, D. Grigoriev, Excitable media store and transfer complicated information via topological defect motion, Communications in Nonlinear Science and Numerical Simulation (2022) 106844.